In order to protonate the metal–metal bond,[12] we added concentrated $HClO_4$ to a solution of complexes III and IV, but the starting material remained unchanged. This is attributed to a low basicity of these complexes.

Addition of Alkynes to Substituted Dinuclear Iridium Complexes. In contrast with the case of complex I, addition of 1 equiv of C_4F_6 or $C_2(CO_2CH_3)_2$ to complex II causes immediate formation of complexes V and VI, respectively. Infrared data, ^1H NMR spectra (Table VIII), molecular weights, and elemental analysis are consistent with the formation of dimetallic complexes formulated: $[Ir_2(\mu\text{-S-}t\text{-Bu})_2(\mu\text{-}C_4F_6)(CO)_2(P(OCH_3)_3)_2]$ (V) and $[Ir_2(\mu\text{-S-}t\text{-Bu})_2(\mu\text{-}C_2(CO_2CH_3)_2(CO)_2(P(OCH_3)_3)_2]$ (VI).

According to ^1H and ^{19}F NMR data, the $-CF_3$ and $-OCH_3$ groups are equivalent and play in these compounds (V and VI) a symmetric role with respect to the pair of iridium atoms. The C–C bond especially is either perpendicular[2] or parallel[3] to the metal–metal axis. By comparison with the trinuclear complexes (III and IV) in which the second proposal is demonstrated, it is admitted here that the alkyne ligand is also σ bonded to both iridium atoms, in the formal II oxidation state, the diamagnetism implying the existence of a metal–metal bond. In fact, the ν_{CO} stretching frequency values are quite consistent with an oxidative addition on a couple of iridium(I) atoms. Furthermore, the low $\nu_{C=C}$ frequency ($\sim$1600 cm^{-1}) in these compounds has never been observed for the C=C bond when perpendicular, and we must admit that it is characteristic of a C=C bond parallel to the metal–metal axis.[3] Although no crystallographic study is yet available, a structure can be tentatively proposed.

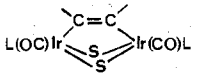

Acknowledgment. We wish to thank Mr. A. Mari for magnetic measurements and the CNRS, DES, and DGRST for their financial support.

Registry No. I, 63312-27-6; II, 63292-76-2; III, 71661-72-8; IV, 71661-71-7; V, 69206-36-6; VI, 71661-70-6.

Supplementary Material Available: A listing of structure factor amplitudes (17 pages). Ordering information is given on any current masthead page.

(12) A. Thorez, A. Maisonnat, and R. Poilblanc, *J. Chem. Soc., Chem. Commun.*, 518 (1977).

Contribution from the Department of Chemistry, The University of Texas at Austin, Austin, Texas 78712

Crystal Structures at −35 °C of Tetraphenylphosphonium (Triphenylphosphino)tetracarbonylmanganate and (Triphenylphosphino)tetracarbonyliron

PAUL E. RILEY and RAYMOND E. DAVIS*

Received March 29, 1979

The structures of $[Ph_4P][Mn(CO)_4PPh_3]$ and $Fe(CO)_4PPh_3$ (Ph = C_6H_5) have been determined by single-crystal X-ray diffraction techniques with three-dimensional data gathered at −35 °C by counter methods. Deep red, block-like single crystals of $[Ph_4P][Mn(CO)_4PPh_3]$ form in monoclinic space group $P2_1/c$ with unit cell constants (at −35 °C) a = 10.735 (3) Å, b = 17.412 (4) Å, c = 20.847 (8) Å, and β = 99.16 (2)°. The calculated density of 1.332 g cm^{-3} is reasonable for four formula weights of $[Ph_4P][Mn(CO)_4PPh_3]$ per unit cell. $Fe(CO)_4PPh_3$ crystallizes as yellow plates in triclinic space group $P\bar{1}$ with unit cell constants (at −35 °C) a = 10.348 (2) Å, b = 10.709 (7) Å, c = 9.809 (6) Å, α = 112.73 (5)°, β = 94.39 (2)°, and γ = 90.12 (2)°. The calculated density of 1.436 g cm^{-3}, assuming two molecules of $Fe(CO)_4PPh_3$ per unit cell, agrees satisfactorily with the measured value of 1.41 g cm^{-3}. Full-matrix least-squares refinements of the structures have converged with conventional R indices (on $|F|$) of 0.077 and 0.061 for $[Ph_4P][Mn(CO)_4PPh_3]$ and $Fe(CO)_4PPh_3$, respectively, using (in the same order) the 4189 and 3961 symmetry-independent reflections with $I_o > 2.0\sigma(I_o)$. In each metal complex the PPh_3 ligand occupies an axial position of a distorted trigonal bipyramid, such that the resulting ML_4L' complexes exhibit approximate C_{3v} symmetry. The average lengths of the M–C bonds in these ML_4L' structures are substantially shorter than those of the parent ML_5 complexes and are equal despite differences in charge and metal atom size. In the Mn structure the axial Mn–C bond shows the larger contraction from the value determined for the unsubstituted complex, suggesting that the PPh_3 substituent exerts a trans stabilizing influence upon the axial CO ligand. In $[Mn(CO)_4PPh_3]^-$, the equatorial Mn–C distances are equal to the corresponding distances in $[Mn(CO)_5]^-$, implying that the π-acceptor orbitals of the equatorial CO ligands are already nearly saturated from the negative charge of the complex. The changes in bond lengths upon phosphine substitution are consistent with the changes in carbonyl stretching force constants and with the reluctance of $[Mn(CO)_4PPh_3]^-$ to undergo additional phosphine substitution. In the two Fe complexes, the equatorial Fe–C bonds show the larger contraction upon phosphine substitution, suggesting that in $Fe(CO)_5$ the π-acceptor orbitals of these CO ligands are not saturated.

Introduction

It has long been established that for trigonal-bipyramidal molecules which possess five equivalent ligands a difference between axial and equatorial bond lengths is generally observed. The explanations offered for this, (1) repulsions between valence shell electron pairs and/or (2) repulsions between valence shell electrons and electrons of partially filled d shells of transition metal atoms (i.e., nonspherical d-electron clouds), have been discussed at length elsewhere.[1,2] Low-spin d^7, d^8, and d^9 metal complexes are of particular interest, because for trigonal-bipyramidal geometry the metal d_{z^2} orbital is either empty or half-filled. Hence, such electron clouds are oblate ellipsoidal, favoring axial bonds which are shorter than equatorial bonds. Furthermore, within an isoelectronic series of trigonal-bipyramidal transition metal complexes of the form ML_5, it has been noted that the difference between axial and equatorial bond lengths decreases with decreasing charge on the metal,[3,4] presumably a result of increased d-electron–valence shell electron repulsion.

(1) R. J. Gillespie, *J. Chem. Soc.*, 4672, 4679 (1963).
(2) A. R. Rossi and R. Hoffmann, *Inorg. Chem.*, **14**, 365 (1975).
(3) B. A. Frenz and J. A. Ibers in "The Biennial Review of Chemistry, Chemical Crystallography", J. M. Robertson, Ed., Medical and Technical Publishing Co., Aylesburg, England, 1972, Chapter 2, and references therein.
(4) B. A. Frenz and J. A. Ibers, *Inorg. Chem.*, **11**, 1109 (1972).

0020-1669/80/1319-0159$01.00/0

In the case of trigonal-bipyramidal transition metal–carbonyl complexes, it has been observed that upon replacement of one CO ligand by a strongly σ-donating/weakly π-accepting ligand, such as $P(C_6H_5)_3$, additional CO replacement becomes more difficult.[5,6] This has been attributed to the greater availability of π-electron density for the remaining (strongly π bonding) CO groups, the effects of which are detectable spectroscopically[7,8] and structurally. For example, Ibers et al.[5] have examined the structural consequences of phosphine substitution for three carbonyl complexes of the form $Mn(CO)_{4-n}(NO)(P(C_6H_5)_3)_n$ (n = 0–2), in which the mode of bonding of NO and CO ligands is very similar. It was noted that while initial phosphine substitution (n = 1) significantly diminished the Mn–C (and Mn–N) bond lengths, additional phosphine substitution, as implied by the reactivity data alluded to above, produced further but proportionally smaller decreases in Mn–C (and Mn–N) bond lengths. Somewhat later, Frenz and Ibers[4] determined the crystal structure of the parent carbonyl complex $[Mn(CO)_5]^-$, which may be regarded as isoelectronic with the nitrosyl complexes.

We report here the crystal structure of $[P(C_6H_5)_4][Mn(CO)_4P(C_6H_5)_3]$, an important member of this series of Mn–carbonyl complexes. We also report the crystal structure of the neutral, and hence isoelectronic, iron–phosphine complex, $Fe(CO)_4P(C_6H_5)_3$, which completes the small set of d^8 transition metal–carbonyl complexes of the form $[M(CO)_{5-n}(P(C_6H_5)_3)_n]^m$ (M = Mn, Fe; n = 0, 1; m = –1, 0), in which the effects of carbonyl replacement and charge variation upon structural parameters may be examined. (Details of the crystal structure of the closely related iron complex, $Fe(CO)_4PH(C_6H_5)_2$, have been published by other workers.[9])

Experimental Section

A sample of $[Ph_4P][Mn(CO)_4PPh_3]$ (Ph represents C_6H_5), which had been recrystallized twice from acetonitrile, was provided by Professor Mark Wrighton. From this sample a suitable deep red, isometric single crystal of this slightly unstable compound was attached to a glass fiber and then transferred to a Syntex $P2_1$ automated diffractometer, where it was maintained in a stream of cold (–35 °C), dry nitrogen during the course of all crystallographic experiments. Preliminary examination of the crystal with the diffractometer indicated monoclinic symmetry consistent with space group $P2_1/c$ (No. 14). Crystal data and data collection details are summarized in Table I. The measured X-ray diffraction intensities were reduced and assigned standard deviations (with p = 0.02) as described previously.[10]

A sample of $Fe(CO)_4PPh_3$ was obtained from Professor Rowland Pettit. Excellent plate-like, yellow single crystals were obtained by slow evaporation of a methanol/acetone (1:1.5 by volume) solution. Oscillation and Weissenberg photographs of a specimen cut from a large plate suggested symmetry no higher than that of the triclinic system (space group $P1$ (No. 1) or $P\bar{1}$ (No. 2)). Crystal data and data collection details may be found in Table I. The data were reduced as before and corrected for absorption.

Solution and Refinement of the Structures

Both structures were solved by standard heavy-atom procedures and then refined by full-matrix least-squares methods.[11] The function minimized in refinement is $\sum w(|F_o| - |F_c|)^2$, where the weight w is $\sigma(|F_o|)^{-2}$, the reciprocal square of the standard deviation of each observation, $|F_o|$. Neutral atom scattering factors for Fe, Mn, P, O, C,[12] and H[13] were used in these calculations, and the real ($\Delta f'$) and imaginary ($\Delta f''$) corrections[12] for anomalous scattering were applied to the Fe, Mn, and P scattering curves.

$[Ph_4P][Mn(CO)_4PPh_3]$. Full-matrix least-squares convergence was attained, using only those 4189 data with $I_o/\sigma(I_o) > 2.0$ for a model in which the phenyl rings were treated as rigid groups of D_{6h} symmetry and nonphenyl ring atoms as ellipsoids, with $R = \sum||F_o| - |F_c||/\sum|F_o| = 0.077$, $R_w = [\sum w(|F_o| - |F_c|)^2/\sum w|F_o|^2]^{1/2} = 0.063$, and a standard deviation of an observation of unit weight $= [\sum w(||F_o| - |F_c||)^2/(m - s)]^{1/2} = 2.12$ for m = 4189 observations and s = 184 variables. Inspection of the data revealed no indication of secondary extinction.

Table I. Crystallographic Summary

	$[Ph_4P][Mn(CO)_4PPh_3]$	$Fe(CO)_4PPh_3$
	Crystal Data at –35 °C[a]	
a, Å	10.735 (3)	10.348 (2)
b, Å	17.412 (4)	10.709 (7)
c, Å	20.847 (8)	9.809 (6)
α, deg	90	112.73 (5)
β, deg	99.16 (2)	94.39 (2)
γ, deg	90	90.12 (2)
V, Å^3	3847 (4)	999 (2)
d_{measd}, g cm^{-3} (19 °C)	...[b]	1.41[c]
d_{calcd}, g cm^{-3} (–35 °C)	1.332	1.436
empirical formula	$C_{46}H_{35}MnO_4P_2$	$C_{22}H_{15}FeO_4P$
fw	768.66	430.18
cryst system	monoclinic	triclinic
systematic absences	$h0l$, $l = 2n + 1$ $0k0$, $k = 2n + 1$	none
space group	$P2_1/c$ (No. 14)	$P1$ (No. 1) or $P\bar{1}$ (No. 2)[d]
Z	4	2
F(000), electrons	1592	440
	Data Collection at –35 °C[e]	
radiation (Mo Kα), Å	0.71069	0.71069
mode	ω scan, recentered automatically after each batch of 1000 reflections	
scan range	symmetrically over 1.0° about $K\alpha_{1,2}$ max	symmetrically over 1.2° about $K\alpha_{1,2}$ max
background	offset 1.0 and –1.0° in ω from $K\alpha_{1,2}$ maximum	
scan rate, deg min^{-1}	variable, 2.0–5.0	
check reflctns	4 remeasured after every 96 reflections; analyses[f] of these data indicated overall decreases in intensity of 2 and 1%, respectively, for which the appropriate corrections were applied	
2θ range, deg	4.0–50.0	4.0–55.0
total reflctns measd	6763	4604
data cryst dimens, mm	0.18 × 0.28 × 0.32	0.18 × 0.33 × 0.66
data cryst faces	(100), ($\bar{1}$00), (010), (0$\bar{1}$0) and 2 faces obtained by cutting	(100), ($\bar{1}$00), (010), (0$\bar{1}$0) and 2 faces obtained by cutting
abs coeff, μ(Mo Kα), cm^{-1}	4.89	8.81
transmission factor range	0.80–0.92[g]	0.74–0.86

[a] Unit cell parameters were obtained by least-squares refinement of the setting angles of 45 reflections with $15.4 < 2\theta < 18.5°$ for $[Ph_4P][Mn(CO)_4PPh_3]$, and 60 reflections with $25.3 < 2\theta < 30.0°$ for $Fe(CO)_4PPh_3$. [b] Due to air-instability an experimental density was not obtained. [c] Flotation in aqueous $ZnCl_2$. [d] Shown by successful refinement to be $P\bar{1}$ (see text). [e] Syntex $P2_1$ autodiffractometer equipped with a graphite monochromator and a Syntex LT-1 inert-gas low-temperature delivery system. [f] W. H. Henslee and R. E. Davis, *Acta Crystallogr., Sect. B*, **31**, 1511 (1975). [g] Data were not corrected for absorption. The estimated transmission factors are based upon the extreme dimensions of the data crystal.

(5) B. A. Frenz, J. H. Enemark, and J. A. Ibers, *Inorg. Chem.*, **8**, 1288 (1969), and references therein.
(6) M. Wrighton, personal communication.
(7) D. J. Darensbourg, *Inorg. Chim. Acta*, **4**, 597 (1970).
(8) D. J. Darensbourg, H. H. Nelson, III, and C. L. Hyde, *Inorg. Chem.*, **13**, 2135 (1974).
(9) B. T. Kilbourn, U. A. Raeburn, and D. T. Thompson, *J. Chem. Soc. A*, 1906 (1969).
(10) P. E. Riley and R. E. Davis, *Acta Crystallogr., Sect. B*, **32**, 381 (1976).
(11) A listing of principal computer programs used in these studies is provided in ref 10.
(12) "International Tables for X-Ray Crystallography", Vol. IV, Kynoch Press, Birmingham, England, 1974.
(13) R. F. Stewart, E. R. Davidson, and W. T. Simpson, *J. Chem. Phys.*, **42**, 3175 (1965).

Table II

(a) Fractional Coordinates and Anisotropic Thermal Parameters ($\times 10^3$) for Nongroup Atoms of $[Ph_4P][Mn(CO)_4PPh_3]$[a]

atom	x	y	z	U_{11}	U_{22}	U_{33}	U_{12}	U_{13}	U_{23}
Mn[b]	0.24719 (8)	0.25468 (5)	0.49096 (4)	350 (5)	346 (5)	275 (5)	−10 (5)	60 (4)	7 (5)
P(1)[b]	0.37669 (15)	0.27844 (9)	0.41853 (7)	389 (10)	340 (10)	247 (8)	−22 (8)	54 (7)	−21 (7)
P(2)[b]	−0.17448 (15)	0.09665 (9)	0.73625 (8)	386 (10)	368 (10)	354 (9)	14 (8)	61 (8)	62 (8)
O(1)	0.0760 (4)	0.2503 (3)	0.5885 (2)	58 (3)	103 (4)	54 (3)	−20 (3)	31 (3)	−8 (3)
O(2)	0.2505 (5)	0.0867 (3)	0.4696 (2)	98 (4)	27 (3)	66 (3)	−8 (3)	16 (3)	−7 (3)
O(3)	0.0492 (5)	0.3480 (3)	0.4132 (3)	64 (4)	73 (4)	95 (4)	31 (3)	−11 (3)	22 (3)
O(4)	0.4571 (4)	0.3106 (3)	0.5891 (2)	58 (3)	85 (4)	35 (3)	−29 (3)	−5 (2)	−11 (3)
C(1)	0.1445 (6)	0.2498 (4)	0.5510 (3)	48 (4)	57 (4)	44 (4)	−14 (4)	3 (3)	−5 (4)
C(2)	0.2486 (6)	0.1527 (4)	0.4767 (3)	47 (4)	56 (5)	37 (4)	3 (4)	10 (3)	4 (3)
C(3)	0.1278 (7)	0.3108 (4)	0.4426 (3)	56 (5)	45 (4)	53 (4)	−0 (4)	9 (4)	−2 (3)
C(4)	0.3736 (6)	0.2898 (4)	0.5506 (3)	51 (4)	49 (4)	35 (4)	−1 (3)	24 (3)	6 (3)

(b) Group Parameters for $[Ph_4P][Mn(CO)_4PPh_3]$[a]

group[c]	x_0	y_0	z_0	ϕ	θ	ρ
Ph(1)	0.3817 (4)	0.3802 (2)	0.3920 (2)	3.125 (3)	−2.882 (2)	−1.626 (3)
Ph(2)	0.3499 (3)	0.2302 (2)	0.3391 (1)	−0.518 (5)	−1.981 (2)	−0.620 (5)
Ph(3)	0.5433 (3)	0.2550 (2)	0.4476 (2)	1.298 (2)	2.903 (2)	2.940 (3)
Ph(4)	−0.1637 (4)	0.1976 (2)	0.7505 (2)	3.136 (3)	3.001 (2)	1.470 (2)
Ph(5)	−0.3261 (3)	0.0740 (2)	0.6921 (2)	−1.263 (2)	−2.631 (2)	−2.889 (3)
Ph(6)	−0.0570 (4)	0.0717 (3)	0.6885 (2)	1.269 (4)	−2.384 (3)	−2.463 (4)
Ph(7)	−0.1538 (4)	0.0430 (2)	0.8101 (2)	0.209 (4)	2.115 (2)	2.684 (4)

[a] See Figure 1 for identity of the atoms and groups. P(2) represents the phosphorus atom of the $[Ph_4P]^+$ ion. Numbers in parentheses throughout the table are the estimated standard deviations in the units of the least significant digits. The U_{ij} are the mean-square amplitudes of vibration in $Å^2$ from the general temperature expression $\exp[-2\pi^2(U_{11}h^2a^{*2} + U_{22}k^2b^{*2} + U_{33}l^2c^{*2} + 2U_{12}hka^*b^* + 2U_{13}hla^*c + 2U_{23}klb^*c^*)]$. [b] For the Mn and P atoms the anisotropic thermal parameters are given $\times 10^4$. [c] For a description of these group parameters see: R. Eisenberg and J. A. Ibers, *Inorg. Chem.*, 4, 773 (1965). Angular coordinates are in radians. The internal coordinate system of a phenyl ring has been defined elsewhere: P. E. Riley and R. E. Davis, *Acta Crystallogr., Sect. B*, 31, 2928 (1975).

Table III

(a) Fractional Coordinates and Anisotropic Thermal Parameters ($\times 10^3$) for Nongroup Atoms of $Fe(CO)_4PPh_3$[a]

atom	x	y	z	U_{11}	U_{22}	U_{33}	U_{12}	U_{13}	U_{23}
Fe[b]	0.15050 (5)	0.29720 (5)	0.26787 (6)	282 (3)	330 (3)	313 (3)	19 (2)	−8 (2)	145 (2)
P[b]	0.28779 (9)	0.18509 (9)	0.36425 (10)	263 (4)	298 (5)	274 (4)	1 (4)	7 (3)	126 (4)
O(1)	−0.0347 (3)	0.4361 (4)	0.1384 (4)	67 (2)	69 (2)	72 (2)	17 (2)	−19 (2)	36 (2)
O(2)	0.3576 (3)	0.4972 (3)	0.3042 (4)	57 (2)	46 (2)	76 (2)	−15 (2)	−5 (2)	29 (2)
O(3)	0.1295 (3)	0.0596 (3)	−0.0141 (3)	54 (2)	52 (2)	41 (2)	0 (1)	1 (1)	5 (1)
O(4)	−0.0123 (3)	0.3388 (4)	0.5142 (4)	42 (2)	80 (2)	58 (2)	8 (2)	18 (2)	26 (2)
C(1)	0.0369 (4)	0.3830 (4)	0.1900 (5)	44 (2)	42 (2)	48 (2)	4 (2)	−4 (2)	17 (2)
C(2)	0.2781 (4)	0.4197 (4)	0.2925 (4)	41 (2)	35 (2)	40 (2)	4 (2)	−2 (2)	18 (2)
C(3)	0.1366 (4)	0.1514 (4)	0.0970 (4)	32 (2)	42 (2)	38 (2)	0 (2)	−2 (2)	18 (2)
C(4)	0.0512 (4)	0.3210 (4)	0.4177 (4)	30 (2)	44 (2)	45 (2)	5 (2)	1 (2)	18 (2)

(b) Group Parameters for $Fe(CO)_4PPh_3$[a]

group[c]	x_0	y_0	z_0	ϕ	θ	ρ
Ph(1)	0.2460 (2)	0.0045 (2)	0.3038 (3)	−0.271 (1)	−2.846 (2)	2.937 (2)
Ph(2)	0.4557 (2)	0.1883 (3)	0.3182 (3)	1.688 (2)	−2.813 (1)	1.811 (2)
Ph(3)	0.3024 (3)	0.2473 (2)	0.5671 (2)	1.268 (12)	1.688 (2)	−2.925 (12)

[a] See Figure 2 for identity of the atoms and groups. Numbers in parentheses throughout the table are the estimated standard deviations in the units of the least significant digits. The U_{ij} expression is given in the caption of Table II. [b] For the Fe and P atoms the anisotropic thermal parameters are given $\times 10^4$. [c] See the caption of Table II for a description of the group parameters.

A structure factor calculation with all 6763 data measured during data collection gave R and R_w values of 0.127 and 0.066, respectively.

In the final cycle of refinement all shifts in nongroup and group atom parameters were less than 2 and 33%, respectively, of a corresponding estimated standard deviation (esd). The largest peaks in a final difference Fourier map were less than 1.0 e $Å^{-3}$ and were primarily associated with anisotropy of the carbonyl groups.

$Fe(CO)_4PPh_3$. Since satisfactory least-squares refinement of this structure was achieved in the centrosymmetric space group $P\bar{1}$, refinement in the noncentrosymmetric space group $P1$ was judged unnecessary. Convergence was reached with R, R_w, and standard deviation of an observation of unit weight indices of 0.061, 0.071, and 3.67, respectively, for $m = 3961$ observations (with $I_o/\sigma(I_o) > 2.0$) and $s = 127$ variables. Calculation of structure factors using all 4604 data measured during data collection yielded R and R_w indices of 0.070 and 0.071, respectively. In the last cycle of refinement the largest shifts in nongroup and group atomic parameters were 16 and 41% of a corresponding esd. There was no evidence of secondary extinction in the data set. The largest peaks in a final difference electron density map were no greater than 0.4 e $Å^{-3}$.

Table II presents atomic positional and thermal parameters, with corresponding esd's as estimated from the least-squares inverse matrix, for the structure of $[Ph_4P][Mn(CO)_4PPh_3]$; the equivalent information for the structure of $Fe(CO)_4PPh_3$ is given in Table III. Tabulations of observed and calculated structure factor amplitudes for both crystal structures are available.[14]

Discussion

The crystal structures of $[Ph_4P][Mn(CO)_4PPh_3]$ and $Fe(CO)_4PPh_3$ consist of discrete ions or molecules with no unusual intermolecular contacts. The molecular geometry of the $[Ph_4P]^+$ ions is approximately tetrahedral, with P–C bond lengths of 1.838 (3), 1.841 (4), and 1.860 (4) Å and C–P–C bond angles ranging from 100.1 (2) to 119.8 (2)°. Figures 1 and 2 provide stereoscopic views of the $[Mn(CO)_4PPh_3]^-$

(14) Supplementary material.

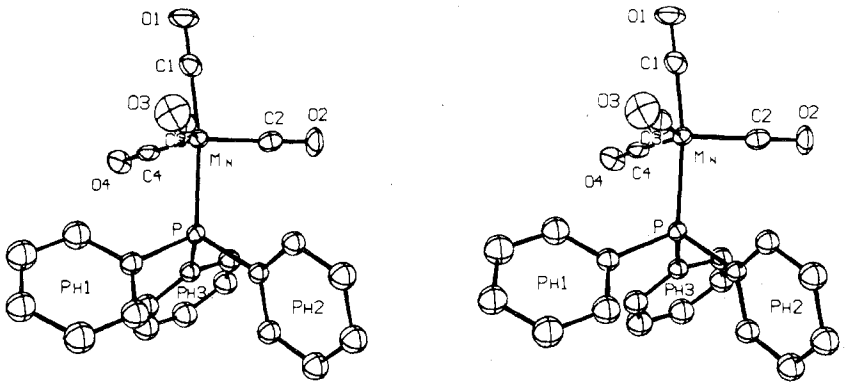

Figure 1. Stereoscopic view of the $[Mn(CO)_4PPh_3]^-$ ion, illustrating the atom numbering scheme. Nonhydrogen atoms are shown as ellipsoids of 30% probability.

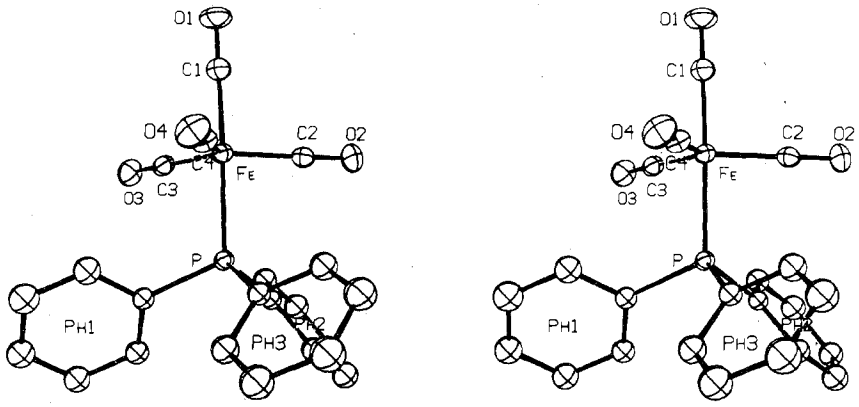

Figure 2. Stereoscopic view of the $Fe(CO)_4PPh_3$ molecule, illustrating the atom numbering scheme. Nonhydrogen atoms are shown as ellipsoids of 30% probability.

and $Fe(CO)_4PPh_3$ complexes and indicate the atom numbering scheme used herein. As may be seen from these figures and from an examination of the bond distances and angles given in Table IV, each complex possesses approximate C_{3v} symmetry with the PPh_3 ligand occupying an axial position, in agreement with structural studies of other substituted transition metal–carbonyl trigonal-bipyramidal complexes and consistent with the generalization[2,15] that the more strongly π-accepting ligands (CO rather than PPh_3) prefer equatorial sites (especially with d^8 metals), so that π back-bonding may be optimized.

Structure of $[Mn(CO)_4PPh_3]^-$. The average axial and equatorial bond lengths in $[Mn(CO)_5]^-$ are 1.820 (14) and 1.798 (15) Å, respectively, distances which do not differ significantly, but, when compared to the corresponding values for other d^8 trigonal-bipyramidal ML_5 complexes[2-4] (in particular see discussion in ref 4), are in accord with the observation that within an isoelectronic series, an increase in the negative charge on the metal atom promotes elongation of the axial bonds in comparison to the equatorial bonds, presumably as a consequence of increased d electron–ligand repulsions. In $[Mn(CO)_4PPh_3]^-$, the Mn–C bond lengths are equal (equatorial Mn–C distances average 1.795 (6) Å and the four Mn–C distances average 1.796 (5) Å[16]) and are also equal to the equatorial Mn–C distances in $[Mn(CO)_5]^-$. Although comparison of the axial and equatorial distances in $[Mn(CO)_5]^-$ and $[Mn(CO)_4PPh_3]^-$ indicates that replacement of one CO ligand (at an axial site) by the strongly σ-donating/weakly π-accepting PPh_3 ligand has indeed strengthened the bonding between Mn and the remaining (π bonding) CO ligands, this enhancement has been nearly restricted to the axial Mn–C bond, its length having decreased by 0.023 (20) Å from its value in $[Mn(CO)_5]^-$. A similar axial shortening (0.03 Å) is apparent upon examination of the crystal structures of $Mn(CO)_4(NO)$ and $Mn(CO)_3(NO)(PPh_3)$.[5] In these complexes, in which NO occupies an equatorial position, phosphine substitution results in substantial decreases in both axial and equatorial Mn–C distances. (Unfortunately, due to disorder of the equatorial ligands in the PPh_3-containing structure, assessment of these changes is not satisfactory.) In contrast, phosphine substitution in the parent anion to give $[Mn(CO)_4PPh_3]^-$ produces a significant decrease only in the remaining Mn–C axial bond length; i.e., the equatorial Mn–carbonyl bonds seemingly do not profit from the increase in electron density on Mn resulting from this substitution. This is not unexpected upon comparison of the force constants derived from the stretching frequencies of the C–O bonds of $[Mn(CO)_5]^-$ and $[Mn(CO)_4PPh_3]^-$ (see Table V). Upon phosphine substitution the stretching force constant for the axial CO ligand decreases by 0.92 mdyn Å^{-1} and that for the equatorial CO groups by 0.58 mdyn Å^{-1}. Also as shown in Table V, the axial and equatorial force constants of $[Mn(CO)_4PPh_3]^-$ differ by less than those of $[Mn(CO)_5]^-$, in

(15) S. A. Goldfield and K. N. Raymond, *Inorg. Chem.*, **13**, 770 (1974).
(16) An average bond length, $\bar{l}$, for n bond lengths is given by $\bar{l} = \sum l_i/n$, and its standard deviation as $\sigma(\bar{l}) = [\sum(l_i - \bar{l})^2/(n-1)]^{1/2}$.
(17) C. D. Pribula and T. L. Brown, *J. Organomet. Chem.*, **71**, 415 (1974).
(18) M. Y. Darensbourg, D. J. Darensbourg, D. Burns, and D. A. Drew, *J. Am. Chem. Soc.*, **98**, 3127 (1976).
(19) J. H. Enemark and J. A. Ibers, *Inorg. Chem.*, **7**, 2339 (1968).
(20) J. H. Enemark and J. A. Ibers, *Inorg. Chem.*, **6**, 1575 (1967).
(21) A. W. Hanson, *Acta Crystallogr.*, **18**, 502 (1962).
(22) B. Beagley, D. W. J. Cruickshank, P. M. Pinder, A. G. Robiette, and G. M. Sheldrick, *Acta Crystallogr., Sect. B*, **25**, 737 (1969).
(23) G. Bor, *Inorg. Chim. Acta*, **3**, 191 (1969).
(24) M. B. Smith and R. Bau, *J. Am. Chem. Soc.*, **95**, 2388 (1973).
(25) M. Y. Darensbourg, D. J. Darensbourg, and H. L. C. Barros, *Inorg. Chem.*, **17**, 297 (1978).

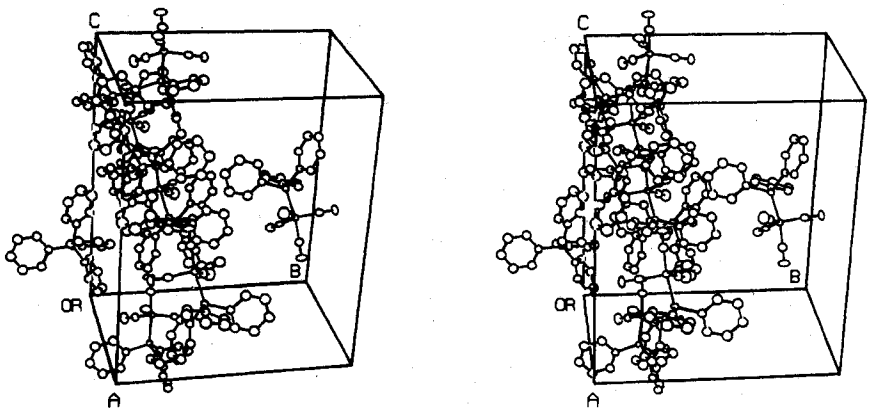

Figure 3. Stereoscopic view of the environment of a $[Mn(CO)_4PPh_3]^-$ ion. Atoms are shown as ellipsoids of 30% probability; hydrogen atoms have been omitted for clarity.

Table IV. Interatomic Distances (Å) and Angles (deg)[a]

	$[Mn(CO)_4PPh_3]^-$ [b]	$Fe(CO)_4PPh_3$ [c]
M-P	2.248 (2)	2.244 (1)
M-C(1)	1.797 (6)	1.795 (4)
M-C(2)	1.801 (7)	1.796 (4)
M-C(3)	1.789 (7)	1.792 (4)
M-C(4)	1.796 (6)	1.796 (4)
C(1)-O(1)	1.157 (7)	1.139 (6)
C(2)-O(2)	1.160 (8)	1.135 (5)
C(3)-O(3)	1.161 (8)	1.149 (5)
C(4)-O(4)	1.162 (8)	1.150 (5)
P-C(11)	1.860 (4)	1.830 (2)
P-C(21)	1.838 (3)	1.832 (2)
P-C(31)	1.841 (4)	1.832 (2)
P-M-C(1)	172.0 (2)	178.3 (1)
P-M-C(2)	92.8 (2)	89.4 (1)
P-M-C(3)	89.2 (2)	88.9 (1)
P-M-C(4)	85.6 (2)	88.2 (1)
C(1)-M-C(2)	95.2 (3)	92.3 (2)
C(1)-M-C(3)	87.4 (3)	90.3 (2)
C(1)-M-C(4)	90.8 (3)	90.9 (2)
C(2)-M-C(3)	118.0 (3)	117.2 (2)
C(2)-M-C(4)	115.1 (3)	119.0 (2)
C(3)-M-C(4)	126.8 (3)	123.6 (2)
M-C(1)-O(1)	176.5 (6)	178.9 (4)
M-C(2)-O(2)	177.9 (5)	178.0 (4)
M-C(3)-O(3)	177.7 (6)	178.3 (4)
M-C(4)-O(4)	178.1 (6)	178.7 (4)
M-P-C(11)	115.2 (1)	114.1 (1)
M-P-C(21)	119.8 (1)	114.5 (1)
M-P-C(31)	114.2 (1)	115.2 (1)
C(11)-P-C(21)	100.1 (2)	104.0 (1)
C(11)-P-C(31)	103.7 (2)	104.2 (1)
C(21)-P-C(31)	101.5 (2)	103.5 (1)

[a] Numbers in parentheses are the estimated standard deviations in the least significant digits. "M" represents Mn or Fe. [b] See Figure 1 for identity of the atoms. [c] See Figure 2 for identity of the atoms.

agreement with the observed differences in Mn–C bond lengths in these two complexes. Furthermore, the stretching force constant for the equatorial CO groups of $[Mn(CO)_4PPh_3]^-$ is substantially smaller than those of the other CO groups given in Table V, implying considerable metal–carbonyl back-bonding in this substituted Mn species.

The true distortion of the structure from C_{3v} symmetry is evident from an examination of the bond angles about the metal. The three equatorial C–Mn–C angles of 115.1, 118.0, and 126.8° differ significantly from the idealized value of 120° and exhibit a pattern similar to that in $[Mn(CO)_5]^-$. However, unlike $[Mn(CO)_5]^-$ in which the shortest equatorial Mn–C distance is opposite the largest equatorial bond angle, the longest equatorial bond (Mn–C(2)) is opposite the largest equatorial bond angle (C(3)–Mn–C(4)) in $[Mn(CO)_4PPh_3]^-$. Although the Mn–C(2) distance does not differ significantly from the other Mn–C bond distances, it is interesting that both axial bonds (Mn–C(1) and Mn–P) are bent away from C(2) (C(1)–Mn–C(2) = 95.2° and P–Mn–C(2) = 92.8°), toward the widest equatorial angle (C(3)–Mn–C(4)). That is, the structure of $[Mn(CO)_4PPh_3]^-$ (at least in the solid state) is distinctly distorted toward square pyramidal, with C(2) (and its O atom) occupying the "apical" position. In $[Mn(CO)_5]^-$, however, the C–Mn–C axial bond angles (two molecules per asymmetric unit) are within 2° of linearity; hence the molecules are virtually trigonal bipyramidal.

The least-squares plane computed with the positions of the equatorial carbon atoms (Table VI) reveals that Mn lies slightly out of this plane (by 0.03 Å), away from PPh_3, an effect which is common to numerous axially substituted trigonal-bypyramidal ML_4L' complexes.[26-30] In addition to attributing this bending of the equatorial CO ligands to steric interactions, it has also been ascribed to at least two other factors: (1) rehybridization of the orbitals of the metal M, which results in a decrease of the repulsions between electron pairs of M and L′ (PPh_3) atoms and a concomitant enhancement of the overlap of filled orbitals of the metal with acceptor orbitals of the equatorial ligands,[29,30] and (2) significant donation of electron density from the σ_z orbitals of L′ into the $2\pi_y$ orbitals of the equatorial carbonyl ligands.[7] The bending of the equatorial ligands toward L′ is then expected to increase metal–equatorial carbonyl orbital overlap. In $[Mn(CO)_5]^-$, incidentally, the Mn atoms do not deviate significantly from the plane of the carbonyl carbon atoms.

Structure of $Fe(CO)_4PPh_3$. The structure of $Fe(CO)_5$ as determined with electron diffraction data[22] possesses axial and equatorial Fe–C bond lengths of 1.806 (5) and 1.833 (4) Å, respectively, distances which differ in the opposite manner from those of $[Mn(CO)_5]^-$. These results, however, are consistent with the view that within a series of isoelectronic trigonal-bipyramidal transition metal complexes a decrease in negative charge on the metal should produce a lengthening of equatorial bonds compared to axial bonds. As in $[Mn(CO)_4PPh_3]^-$, phosphine substitution has yielded a trigonal-bipyramidal iron complex with equivalent metal–carbon bond lengths (equatorial Fe–C distances average 1.795 (2) Å and the four Fe–C distances average 1.795 (2) Å), which interestingly are equal to the Mn–C bond distances in $[Mn(CO)_4PPh_3]^-$. This equivalence of metal–carbonyl bond lengths for charged and uncharged ML_4L' complexes contradicts the results obtained

(26) K. Emerson, P. R. Ireland, and W. T. Robinson, *Inorg. Chem.*, **9**, 436 (1970), and references therein.
(27) J. A. Ibers, *Annu. Rev. Phys. Chem.*, **16**, 375 (1965).
(28) P. E. Riley and R. E. Davis, *J. Organomet. Chem.*, **137**, 91 (1977).
(29) T. L. Blundell and H. M. Powell, *J. Chem. Soc. A*, 1685 (1971).
(30) M. J. Bennett and R. Mason, *Nature (London)*, **205**, 760 (1965).

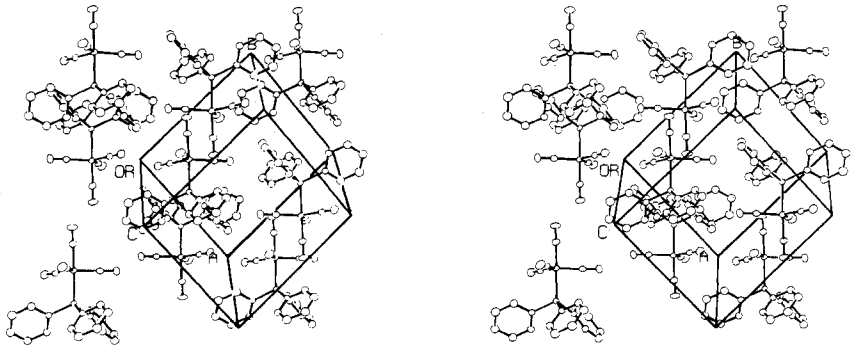

Figure 4. Stereoscopic view of the surroundings of a $Fe(CO)_4PPh_3$ molecule. Atoms are drawn as ellipsoids of 30% probability; hydrogen atoms have been omitted for clarity.

Table V. Metal Carbonyl Bond Lengths (Å) and Carbonyl Stretching Force Constants (mdyn $Å^{-1}$) for Some Trigonal-Bipyramidal Mn(−I) and Fe(0) Complexes

compd	M–C(CO) distances[a]			CO stretching force constants[b]		
	eq	ax	ref	eq	ax	ref
$[Mn(CO)_5]^-$	1.798 (15)	1.820 (14)	4	14.36	15.05	17
$[Mn(CO)_4PPh_3]^-$	1.795 (6)	1.797 (6)	this work	13.78	14.13	18
$Mn(CO)_4(NO)$	1.851 (8)	1.886 (8)	5			
$Mn(CO)_3(NO)PPh_3$	1.798 (10)[c] 1.782 (11)[c] 1.756 (10)[c]	1.833 (11)	19			
$Mn(CO)_2(NO)(PPh_3)_2$	1.77 (2)		20			
$Fe(CO)_5$ X-ray diff	1.795 (20)	1.795 (20)	21	16.41	16.98	23
electron diff	1.833 (4)	1.806 (5)	22			
$Fe(CO)_4PPh_3$	1.795 (4)	1.795 (2)	this work	15.71	16.15	8
$Fe(CO)_4PHPh_2$	1.792 (8)	1.793 (9)	9			
$[Fe(CO)_4(CN)]^-$	1.768 (8)	1.723 (8)	23			
$[Fe(CO)_4H]^-$	1.75 (4)	1.72 (2)	24	14.72	15.02	25

[a] Average distances are reported for complexes with more than one type of M–C bond. Numbers in parentheses are the estimated standard deviations in the least significant digits. [b] Force constants have not been reported for some complexes of this table. [c] Due to disorder equatorial ligands were refined as $^2/_3$CO and $^1/_3$NO.

Table VI. Deviations from Equatorial Least-Squares Planes[a]

atom	dev,[b] Å	atom	dev,[b] Å
	$[Mn(CO)_4PPh_3]^-$		
	$0.7030X + 0.1238Y - 0.7004Z + 5.7786 = 0$		
C(2)*	0	P	2.212 (2)
C(3)*	0	O(2)	−0.008 (5)
C(4)*	0	O(3)	−0.020 (5)
Mn	−0.0298 (8)	O(4)	0.030 (4)
	$Fe(CO)_4PPh_3$		
	$-0.6117X + 0.6923Y - 0.3827Z + 0.2854 = 0$		
C(2)*	0	P	−2.207 (1)
C(3)*	0	O(2)	0.006 (3)
C(4)*	0	O(3)	−0.012 (3)
Fe	0.0359 (6)	O(4)	−0.008 (4)

[a] Orthonormal (Å) coordinate system with axes X, Y, and Z parallel to unit cell vectors a, b, and c^* for the monoclinic crystal system or a, $c^* \times a$, and c^* for the triclinic crystal system. A negative deviation from the plane indicates that the atom with coordinates given in Table II or III lies between the plane and the unit cell origin. See Figures 1 and 2 for identity of the atoms. [b] Numbers in parentheses are estimated standard deviations in the least significant digit.

for an isoelectronic series of ML_5 complexes for which a correlation between charge and relative bond length is probable.[2-5]

However, unlike $[Mn(CO)_4PPh_3]^-$ in which the equatorial Mn–C bonds appear to be unaffected by phosphine substitution, $Fe(CO)_4PPh_3$ exhibits greater bond length contraction at the equatorial sites than at the remaining axial site. As noted earlier, strongly π-accepting ligands (e.g., CO) prefer equatorial sites in trigonal-bipyramidal transition metal complexes.[2,15] Thus the extent of the changes in axial and equatorial bond lengths upon substitution of the predominantly electron-donating PPh_3 group for an electron-accepting CO ligand to form the charged and uncharged ML_4L' complexes are intriguing, if not significant. In the Mn complexes, these differences (see Table V) are 0.023 (20) and 0.003 (21) Å in the axial and equatorial Mn–C distances, respectively, while in the Fe complexes these differences are, in the same order, 0.011 (9) and 0.038 (6) Å. Thus, it appears that because of the negative charge on the metal atom of the Mn complexes the π-acceptor orbitals of the equatorial CO ligands are nearly saturated and that the additional electron density placed on the metal by the PPh_3 substituent cannot be accepted by these ligands. Consequently, the remaining CO ligand at the less favored π-bonding axial site[2,15] is now able to acquire excess electron density, as reflected by the apparent (though not significant), large decrease in axial Mn–C bond length. In the uncharged Fe complexes, however, the π-acceptor orbitals of the equatorial CO ligands apparently are not saturated and hence readily accept the excess electron density placed upon Fe by phosphine substitution. This suggestion has been offered previously as a possible explanation for the structural and reactivity data obtained for the $Mn(CO)_{4-n}(NO)(PPh_3)_n$ (n = 0–2) series.[5] Accompanying these changes in Fe–C bond lengths following PPh_3 substitution are, of course, corresponding decreases in the CO stretching force constants (see Table V; 0.83 and 0.70 mdyn $Å^{-1}$ for axial and equatorial CO ligands, respectively), values which reflect the magnitude of the changes in the corresponding Fe–C bond distances. It is interesting that the larger changes in force constants within each pair of complexes (Mn or Fe) are in the axial carbonyl groups and perhaps indicate a trans-stabilizing influence.[2]

The geometry of $Fe(CO)_4PPh_3$ at least in the solid state is more regular than that of $[Mn(CO)_4PPh_3]^-$. Although the values of the equatorial angles (117.2, 119.0, and 123.6°)

resemble the pattern observed for $[Mn(CO)_5]^-$ and $[Mn(CO)_4PPh_3]^-$, the deviations from C_{3v} symmetry for $Fe(CO)_4PPh_3$ are less severe, i.e., the axial-Fe-equatorial bond angles are close to 90° (88.2-92.3°) and the C(1)-Fe-P angle is essentially linear (178.3°). As shown in Table VI, Fe lies out of the plane of the equatorial carbon atoms and away from the PPh_3 ligand, a feature which is common in trigonal-bipyramidal ML_4L' structures and which was discussed in the preceding section.

Figure 3 illustrates the packing arrangement of the $[Ph_4P]^+$ and $[Mn(CO)_4PPh_3]^-$ ions. Each $[Mn(CO)_4PPh_3]^-$ ion is surrounded by two cations and two anions at distances of ca. 3.25 Å and by an additional two cations and two anions at distances of ca. 3.5 Å. As shown in Figure 4, each $Fe(CO)_4PPh_3$ molecule is surrounded by eight other molecules at distances of ca. 3.5 Å. Neither arrangement corresponds to an easily recognizable type of molecular packing.

Acknowledgment. This work was supported by the Robert A. Welch Foundation (Grant No. F-233). We are also indebted to the National Science Foundation for purchase of the Syntex $P2_1$ diffractometer (Grant No. GP-37028), to Professor Mark Wrighton for supplying crystals of $[Ph_4P][Mn(CO)_4PPh_3]$, and to Professor Rowland Pettit and Charles Sumner for providing a sample of $Fe(CO)_4PPh_3$.

Registry No. $[Ph_4P][Mn(CO)_4PPh_3]$, 71927-68-9; $Fe(CO)_4PPh_3$, 35679-07-3.

Supplementary Material Available: Listings of structure factor amplitudes and fractional coordinates (58 pages). Ordering information is given on any current masthead page.

Contribution from the Departments of Chemistry, Baylor University, Waco, Texas 76703, and Abilene Christian University, Abilene, Texas 79601

Iron-Nitrogen Bond Lengths in Low-Spin and High-Spin Iron(II) Complexes with Poly(pyrazolyl)borate Ligands

J. D. OLIVER,[1a] D. F. MULLICA,[1b] B. B. HUTCHINSON,*[1c] and W. O. MILLIGAN*[1b]

Received July 13, 1979

The structures of bis[hydrotris(1-pyrazolyl)borato]iron(II) (**1**), $C_{18}H_{20}N_{12}B_2Fe$, and bis[hydrotris(3,5-dimethylpyrazolyl)borato]iron(II) (**2**), $C_{30}H_{44}N_{12}B_2Fe$, have been elucidated by single-crystal X-ray diffraction techniques. The iron atom in **1** is in the low-spin state at room temperature, whereas in **2** the iron atom is in the high-spin state at room temperature. Both molecules possess virtual D_{3d} symmetry in the solid state. The average metal-ligand bond distances, ⟨Fe-N⟩, are 1.973 (7) Å for **1** and 2.172 (22) Å for **2**. The ⟨Fe-N⟩ value for the high-spin complex is thus 0.199 Å longer than the similar value for the low-spin complex. This is one of the largest values observed for the bond length expansion between the low-spin and high-spin states. The averages of the independent N-Fe-N bond angles are 88.3 (2)° for **1** and 86.6 (5)° for **2**. Crystal data for **1** are as follows: space group $P2_1/c$; $Z = 4$; $a = 12.258$ (3), $b = 11.606$ (2), $c = 16.518$ (3) Å; $\beta = 107.56$ (2)°; $V = 2240$ Å^3; $R = 5.2\%$ for 1890 reflections. Crystal data for **2** are as follows: space group $P\bar{1}$; $Z = 1$; $a = 8.824$ (3), $b = 10.216$ (4), $c = 10.787$ (4) Å; $\alpha = 116.36$ (3), $\beta = 85.24$ (3), $\gamma = 100.09$ (3)°; $V = 858$ Å^3; $R = 3.9\%$ for 1819 reflections.

Introduction

Beginning in 1966[2] the coordination chemistry of poly(1-pyrazolyl)borate ligands has been the center of exhaustive research. One of the earlier types of complexes studied was of the form $(HBPz_3)_2M$, where M is a divalent metal ion. A crystal structure of one such complex, $(HBPz_3)_2Co$,[3] has appeared. The temperature dependence of the magnetic moment of the complex $(HBPz_3)_2Fe$ (**1**) in chloroform indicated a "spin equilibrium" between the low- and high-spin forms.[4] Spin crossover in the solid state was first implied by the observation of a color change from purple to white upon heating.[5] Magnetic susceptibility and Mössbauer and infrared spectroscopic studies have confirmed this spin crossover at 393 K.[6] Although several Fe(II) compounds are known which exhibit spin-equilibrium characteristics, this Fe(II) complex is unique in that the crossover is from low to high spin and occurs above room temperature. The magnetic properties of a very similar complex, $[HB(C_5H_7N_2)_3]_2Fe$ (**2**), indicated that it is a high-spin complex at room temperature.

Since a change from t_{2g}^6 low-spin state to a $t_{2g}^4e_g^2$ high-spin state is predicted to be accompanied by an expansion of the metal-ligand bond length, accurate X-ray crystal analyses are important to obtain the magnitude and pattern of such changes. An approximate value for the bond-length difference, δ, of 0.12 Å resulted from a structure study[7] of $[Fe(phen)_2(NCS)_2]$ at 295 and 100 K; however, the accuracy of these determinations was poor. The room-temperature structural study[8] of two solvated forms of the α-picolyamine (α-P) complex, $[Fe(\alpha\text{-P})_3]Cl_2$, have yielded a more accurate value of 0.192 Å for δ. In addition to the spin-state difference, a major stereochemical change resulted from a difference in solvation. For the aquated form, the three amine nitrogen atoms occupy a triangular face of the coordination octahedron. In the methanol solvated form, two amine nitrogen atoms and one pyridine nitrogen atom occupy this triangular face. The possibility thus exists that the spin-state difference as well as the stereochemical difference might both contribute to δ. With this in mind we have completed the structural analysis of the complexes **1** and **2** in order to obtain an accurate value for δ in the absence of a stereochemical change.

Experimental Section

Syntheses of **1** and **2** were accomplished by a previously published method.[9] All X-ray measurements were made on a four-circle

(1) (a) On Sabbatical leave from Department of Chemistry, West Texas State University, Canyon, Texas. (b) Baylor University. (c) Abilene Christian University.
(2) S. Trofimenko, *J. Am. Chem. Soc.*, **88**, 1842 (1966).
(3) M. R. Churchill, K. Gold, and C. E. Maw, Jr., *Inorg. Chem.*, **9**, 1597 (1970).
(4) J. P. Jesson, S. Trofimenko, and D. R. Eaton, *J. Am. Chem. Soc.*, **89**, 3158 (1967).
(5) S. Trofimenko, *Acc. Chem. Res.*, **4**, 7 (1971).
(6) B. Hutchinson, L. Daniels, and G. Long, *Chem. Commun.*, in press.
(7) E. Konig and K. J. Watson, *Chem. Phys. Lett.*, **6**, 457 (1970).
(8) A. M. Greenaway and E. Sinn, *J. Am. Chem. Soc.*, **100**, 8080 (1978).
(9) S. Trofimenko, *J. Am. Chem. Soc.*, **89**, 3170 (1967).

0020-1669/80/1319-0165$01.00/0